THE PENNSYLVANIA STATE UNIVERSITY
SCHREYER HONORS COLLEGE

DEPARTMENTS OF ENGINEERING SCIENCE AND MECHANICS
AND CHEMICAL ENGINEERING

# WATER ADSORPTION AND CHARACTERIZATION ON ALKANETHIOL SELF-ASSEMBLED MONOLAYERS ON GOLD

AIMEE TU

Spring 2010

A thesis
submitted in partial fulfillment
of the requirements
for baccalaureate degrees
in Engineering Science and Chemical Engineering
with interdisciplinary honors in Engineering Science and Chemical Engineering

Reviewed and approved* by the following:

Seong H. Kim
Associate Professor of Chemical Engineering
Thesis Supervisor

Christine B. Masters
Assistant Professor of Engineering Science and Mechanics
Honors Adviser

Themis Matsoukas
Professor of Chemical Engineering
Honors Adviser

Judith A. Todd
P. B. Breneman Department Head Chair
Professor, Department of Engineering Science and Mechanics

*Signatures are on file in the Schreyer Honors College and the Engineering Science and Mechanics office.

# ABSTRACT

The water adsorption isotherms on three different functional groups – methyl, carboxylic acid, and hydroxyl terminated alkanethiol SAMs on gold were studied. The water adsorption isotherms were measured with polarization modulation reflection absorption infrared spectroscopy (PM-RAIRS), which gives structural information, but cannot give absolute thickness; quartz crystal microbalance (QCM), which gives the mass gain that can be related to thickness; and ellipsometry, which gives thickness information. While it was desired for more quantitative information to be obtained from QCM and ellipsometry, because of the nature of these techniques, the small amount of molecules adsorbed, and the materials used, the results from these techniques must be mainly taken as qualitative. For QCM, the adsorption of water on the bare quartz surface not covered with SAM interferes with the accurate measurement of the water adsorbed by the SAM-modified surface on the QCM crystal. Meanwhile, the ellipsometer experienced some problems due to laser instability and electrical grounding, so the sensitivity was not good. The ellipsometer gave qualitative trends, but actual thickness could not be determined. However, these three techniques used together provided an idea of the structure and thickness of the water layer adsorbed and the behavior of water on these surfaces. The –$CH_3$ terminated SAM did not adsorb water as the relative humidity was increased. The water on the –COOH terminated SAM has a broad OH stretching peak, indicating different hydrogen bonding behavior. Ionized carboxylic acid groups were also present on the surface, causing a stronger water-surface interaction. The –OH terminated SAM

showed a narrower OH stretching peak, and also a large amount of water (~18 Å) that could not be removed in dry conditions.

# TABLE OF CONTENTS

# LIST OF FIGURES

# ACKNOWLEDGEMENTS

I would like to thank my adviser, Dr. Seong Kim, for the guidance, insight, and support he has provided during this project. I would also like to thank Anna Barnette for mentoring me, as well as the other group members: Erik Hsiao and Laura Bradley for performing the ellipsometry experiments, and Matt Marino, David Marchand, Brandon Veres, and Zach Dilworth for their support. Their contributions helped the project move along, and they were also very enjoyable to work with. I would also like to thank my honors adviser, Dr. Christine Masters, for her support and advice.

# Chapter 1

## Motivation: Water Adsorption Behavior on Surfaces

Water is present on virtually all surfaces due to atmospheric humidity. The interfacial properties of water have important implications in biosensing,[1] atmospheric interactions,[2,3] biological processes,[4] and nanotechnology. Many studies have been done on the behavior of interfacial water on various surfaces; however, the structure of water on these surfaces is still somewhat unknown. Specifically, silicon oxide has been studied vigorously because of its importance in the semiconductor industry. These studies have found that water exhibits solid-like behavior at low relative humidity, but eventually transitions to liquid-like behavior at higher humidities.[5,6] The behavior of interfacial water on surfaces is important to understand, as it can have profound effects on how a device performs.

Self-assembled monolayers (SAMs) can be controlled to produce virtually any surface. SAMs have become important in a wide variety of fields, such as biochemistry, electronics, and electrochemistry. SAMs are characterized by the chemisorptions, or covalent bonding, of molecules to a substrate, thus forming a single layer of molecules on the surface. SAMs are an easy way to control the chemical composition and physical structure of a surface.[7] Because of their dense and stable structure, SAMs have potential applications in corrosion prevention and wear protection.[8] The interfacial properties of SAMs are important in biosensing applications, and water adsorption is particularly relevant due to its ubiquitous presence in most environments. In this work, the water

adsorption on alkanethiols terminated with $CH_3$, OH, and COOH on gold will be examined.

## Methods to Characterize SAMs

Many techniques can be employed to give information about adsorbed molecules on a surface. However, each technique has a limitation and cannot give all of the information of interest. The main techniques examined here are spectroscopy, which offers structural information, acoustic wave, which offers quantitative information about the mass adsorbed, and ellipsometry, which provides quantitative thickness information.

### Infrared Spectroscopy

Molecules vibrate and rotate at specific frequencies corresponding to discrete energy levels (vibrational modes). When the frequency of a specific rotation or vibration is equal to the frequency of the infrared (IR) radiation directed towards the molecule, the molecule absorbs the radiation, which appears as a peak in the spectrum. A sample can be identified by the frequency of the absorption peaks which appear in the spectrum. The size of the peaks is also directly related to the amount of the material present. The exact frequency at which a vibration occurs is determined by the strengths of the bonds involved and the mass of component atoms. Functional groups can be identified using IR, as they are known to show peaks in a certain range of frequencies. This process is known as Infrared Spectroscopy.

***Fourier Transform Infrared Spectroscopy (FTIR)***

Fourier Transform Infrared Spectroscopy (FTIR) uses an interferometer, which produces a unique signal which has all of the infrared frequencies "encoded" into it.[9] The signal can be measured very quickly, which reduces the sampling time. A beamsplitter causes the incoming infrared beam to split into two beams that reflect off of two flat mirrors, one which is stationary, and one which moves a very a short distance. Once reflected off the mirrors, the two beams will recombine and interfere with each other in the beamsplitter. The beam then passes through the sample and is measured by the detector. The interferogram signal is converted to a frequency spectrum by using the Fourier transform.

FTIR is useful because it can identify organic functional groups and can be run in ambient conditions. Measurements can be done in-situ without destruction of the sample. Information about the structure of adsorbed groups (solid-like versus liquid-like water) can be obtained by deconvoluting the broad O-H stretching peak. However, FTIR does have limited surface sensitivity and is typically not quantitative. Also, many materials are opaque to IR radiation, and must be analyzed using other techniques.

***Attenuated Total Reflectance Infrared Spectroscopy (ATR-IR)***

Attenuated Total Reflectance Infrared Spectroscopy (ATR-IR) uses a high-refractive-index crystal to cause "total" reflection. The beam first enters this crystal, then enters into a less dense medium with a lower refractive index. When the angle of incidence is greater than the critical angle, all incident radiation is completely reflected at

the interface, but the beam penetrates a very short distance beyond the interface into the less dense medium before the complete reflection occurs. This penetration is called the evanescent wave, and is on the order of a few micrometers. Its intensity is attenuated by the sample in regions of the IR spectrum where the sample absorbs.[10] The peak positions for ATR-IR are the same as for FTIR, but the relative intensities of the corresponding bands are different. ATR-IR has much of the same advantages and limitations as FTIR. It is able to only probe certain samples, and unfortunately gold is not one of them. However, the natural log of the reflectance is proportional to the distribution of different configurations as well as the total thickness of the adsorbed water layers.[11]

***Polarization Modulation Reflection-Absorption Infrared Spectroscopy (PM-RAIRS)***

Polarization Modulation Reflection-Absorption Infrared Spectroscopy (PM-RAIRS) is an alternative IR technique that is used for the characterization of thin films or monolayers on a metal substrate. IR light is passed through a photo-elastic modulator, which generates alternating linear states of s- and p-polarized light where p refers to parallel polarized radiation and s to perpendicular polarized radiation with respect to the plane of incidence. PM-RAIRS measures two different signals at the same time: the difference spectrum between s- and p-polarized light and the corresponding sum spectrum. The thin layers on metal surfaces interact with p-polarized light, but not with the s-polarized light.

PM-RAIRS is useful because the modulated reflectivity is independent of isotropic adsorption from gas or bulk water, which means atmospheric absorptions

caused by water vapor and carbon dioxide are eliminated.[12] It also has high surface sensitivity, and peak positions not only give an idea of the functional groups on the metal surface but also the structure of the film. However, it is difficult to quantify the amount or thickness of the film from the intensity of the peaks.

**Quartz Crystal Microbalance (QCM)**

Quartz Crystal Microbalance (QCM) measures the mass per unit area by relating it to the change in frequency of a quartz crystal resonator. The frequency change can be related to mass by using the Sauerbrey equation,

$$\Delta f = \frac{-2\Delta m f_0^2}{A\sqrt{\rho_q \mu_q}} = -C_f \Delta m \qquad [1]$$

which relies on a linear sensitivity factor, $C_f$. The mass change can be used along with an assumed density to estimate the thickness of the adsorbed layer. Quartz is subject to the piezoelectric effect, which means that applying an alternating current to the quartz crystal will cause oscillations. The frequency of these oscillations depends on the mass deposited on the crystal – the more mass, the smaller the frequency.

QCM is a very sensitive instrument. A change in temperature of 1°C will result in a frequency change of 8 Hz, which is significant in these experiments, especially when dealing with water adsorption on hydrophobic surfaces. The quartz crystals used for QCM are not completely coated with gold. A portion of the crystal is bare quartz, which is a hydrophilic surface that thiols do not adsorb to. Thus, some of the frequency change that is observed could be due to water adsorption on the quartz surface, which makes it difficult to determine mass and thickness of the adsorbed water layer on the SAM.

**Surface Acoustic Wave (SAW)**

Surface Acoustic Wave (SAW) sensors are similar to QCM, except they utilize the surface acoustic wave mode of propagation, or Rayleigh waves, to sense mass and mechanical properties. Rayleigh waves have a longitudinal and a vertical shear component that can couple with a medium in contact with the device's surfaces. This coupling strongly affects the amplitude and velocity of the wave. The SAW response is considered to be exclusively due to changes in adsorbed mass on the surface between the interdigital transducers (IDTs) used to convert the electrical signal into an acoustic surface wave and vice versa.[1] SAW sensors have a high sensitivity, and corrections for changes due to the bare quartz can be quantified. However, it can easily be influenced by chances in the viscoelastic properties of the surface film. It is also gives no information about the actual identity of the adsorbed film.

**Ellipsometry**

Ellipsometry measures the change of polarization of light upon reflection or transmission, which is determined by the sample's thickness and refractive index. Ellipsometry mainly analyzes the phase information and the polarization state of light. This technique can achieve angstrom resolution, but the sample must be composed of optically homogeneous and isotropic layers. Thus, the surface roughness of samples must be small. Ellipsometry measures two values, $\psi$ and $\Delta$, which represent the amplitude ratio and phase difference between p- and s-polarized light waves, respectively. While single-wavelength ellipsometry uses a monochromatic light source, such as a laser in the visible

light region, spectroscopic ellipsometry (SE) uses broad band light sources, which cover a certain range in the infrared, visible, or ultraviolet spectral region. In SE, ($\psi$,$\Delta$) are measured by changing the wavelength of light.[13] The angle of incidence chosen is very important, as p- and s-polarizations must be able to be distinguished. The angle of incidence varies according to the optical constants of samples. The advantages of ellipsometry are high precision, nondestructive and fast measurement, real-time monitoring, and various characterizations. However, an optical model is necessary in data analysis; this implies indirect characterization and can often be very complicated. Ellipsometry also has low special resolution and has difficulty in the characterization of low absorption coefficients.

**Temperature Programmed Desorption (TPD)**

Temperature Programmed Desorption (TPD) gives information about the binding energy of an adsorbed molecule to a surface by observing the mass of molecules adsorbed and the temperature at which they desorb. TPD can also reveal the amounts of adsorbed molecules on the surface from the intensity of the peaks in the spectrum. The total amount of the adsorbed species is shown by an integral of the spectrum. TPD must be done in a vacuum.

### Molecular Controlled Semiconductor Resistor (MOCSER)

Molecular Controlled Semiconductor Resistor (MOCSER) is a newly developed field effect transistor (FET). It is based on GaAs structure, and small variations in surface charge lead to significant changes in carrier concentration in the conductive layer.[14] MOCSER can be coated with different dielectric layers and keep its sensitivity for processes occurring on top of these layers, so it is useful in detecting changes caused by humidity. However, MOCSER is only sensitive to molecules in contact with the surface, so simultaneous measurements with another technique would be necessary to develop a better idea of what is going on.[2]

## Differences Between SAMs

### Silane SAMs on Silicon

Alkylsilane SAMs require hydroxylated substrates for their formation. Self-assembly occurs because of the formation of polysiloxane, which is connected to surface silanol groups (-SiOH) via Si-O-Si bonds. These types of monolayers have been prepared on silicon oxide, aluminum oxide, quartz, glass, mica, and gold activated by UV-ozone exposure. However, for alkyltrichlorosilane, high quality SAMs are difficult to produce, because the amount of water in solution must be carefully controlled. A study by McGovern et al (1994) suggested a moisture quantity of 0.15 mg/100 mL of solvent as the optimum condition for the formation of densely packed monolayers.[15] Temperature also plays an important role in the formation of these monolayers. There is competition

between the self reactions of hydrolyzed trichlorosilyl groups with each other to form polymers and the reaction of these groups with the surface Si-OH groups to form the monolayer. The reaction to form the SAMs is favored as temperature decreases, which also decreases thermal disorder and results in a better-ordered monolayer.

Many studies have been done to characterize alkyltrichlorosilane monolayers. Work done by Biernbaum et al (1995) showed that introduction of a polar amino group termination resulted in a more disordered monolayer, probably as a result of acid-base reactions with surface silanol groups.[16] Also, the adsorption mechanisms of trichlorosilane and trimethoxysilane groups are different, as octadecyltrimethoxysilane (OTMS) had a higher tilt angle than octadecyltrichlorosilane (OTS). Alkyltrichlorosilanes are still difficult to characterize, since the quality of the monolayer is very sensitive to reaction conditions. Several studies have reported different optimal times for the formation of the SAM, ranging from 3 minutes to over 24 hours. It has also been shown that there were pinholes in OTS monolayers on mica,[17] and some have emphasized that in order to obtain reproducible, good quality films, samples must be prepared under class 100 clean room conditions.[18] These SAMs are more disordered than thiol SAMs probably because for trichlorosilanes, the formed islands are composed of polymerized surfactants, and therefore the mobility is restricted.[8]

Surface modification for these SAMs can be done by either using ω-substituted alkylsilanes, or by surface chemical reactions via nucleophilic substitution. However, both of these methods can disrupt the order of the SAM. Mixed monolayers are also useful for surface engineering, and can be made by tailoring the composition of the immersion solution.

**Alkanethiol SAMs on Gold**

Gold is the most popular material on which thiol SAMs are formed.[7] Gold can be handled in air without the formation of an oxide surface layer, and can withstand harsh chemical treatments that are used to clean it. The smoothness of the metal partially dictates the structure of the monolayer, especially the defect density. Sulfur-containing compounds have a strong affinity for noble metal surfaces. For alkanethiols, the mechanism of binding is thought to be an oxidative addition of the S-H bond followed by reductive elimination of hydrogen, which results in the formation of a thiolate species.[4] These SAMs are known to be stable in air or in contact with water or ethanol for several months, but are damaged at temperatures greater than 70°C or when irradiated with UV light in the presence of oxygen.

Samples of these SAMs can be prepared by immersing the gold substrate in dilute thiol solutions in high purity solvents such as ethanol, tetrahydrofuran, and dichloromethane. The reaction times required to obtain a densely packed monolayer vary from several minutes to several hours. Dense monolayers can assemble quickly, but well-ordered monolayers may take days to form. Thiols with alkyl chains greater than 10 carbons are thought to produce more ordered SAMs than shorter length chains.

**Comparison of SAMs**

While alkylsilane SAMs are more thermally stable than alkanethiols on gold, they are limited by the conditions under which they must be formed, and are often more disordered than alkanethiols on gold. It is also more difficult to introduce different terminal groups with the alkylsilane SAMs, as this can affect the ordering of the molecules. As mentioned later on, the quality of the SAM is very important, as it is difficult to characterize the structure of adsorbed water if water is penetrating into the SAM.

## Water on $SiO_2$

Studies concerning adsorbed water on silicon oxide have yielded interesting findings concerning the structure of adsorbed water layers. Silicon is often studied, as it is important in the semiconductor industry. A silicon ATR crystal was exposed to UV/O3 which is believed to saturate the oxide surface with hydroxyl groups. Asay and Kim (2005) explored the behavior of adsorbed water on amorphous SiO2 using ATR-IR, which gives information about the structure and average thickness of the water layers.[5] The ATR-IR spectra showed three significant peaks in the O-H stretching vibration region: a small sharp peak at 3740 $cm^{-1}$ and two broad peaks at 3230 $cm^{-1}$ and 3400 $cm^{-1}$. It was found that there were three regions in the adsorption isotherm corresponding to icelike water growth, transitional growth, and liquid water growth. Due to the immobilized hydroxyl groups on the surface, the first monolayer of adsorbed water is ordered in an ice-like manner. However, as the relative humidity was increased, a liquid-

like layer began to grow before the growth of the ice-like layer ended, marking the transitional region, which resulted in the growth of only one more layer. As the relative humidity was increased above 60%, the structure of the outermost layer was liquid-like, as it was dominated by thermal motion. The thickness of the adsorbed water layer also began to increase exponentially with RH. Thus, a Type II isotherm was observed for water on silicon oxide.

A closely related study that was performed following the previous one further investigated adsorbed water layers on silicon oxide. The purpose of this study was to look further at the structure of interfacial water on $SiO_2$. As the relative humidity increased, the properties of the adsorbed water changed. At low relative humidities, it was found that the adsorbed water molecules in the solid-like and liquid structures were not randomly oriented.[19] The thickness of the adsorbed layer increases with relative humidity. Also, as the thickness increased, the water molecules lost the order they had at low relative humidity. These conclusions were obtained from looking at data from attenuated total reflectance infrared spectroscopy (ATR-IR) and also calculating the dichroic ratio from these data, which gives information about how the adsorbed water molecules are oriented.

Numerous other studies have been conducted exploring the structure of adsorbed water on silicon. Verdaguer et al. (2007) observed the same Type II isotherm found by Asay et al using XPS.[6] The study also examined how the structure of 4-6 monolayers of water changed with temperature. NEXAFS showed that at -9C, a clear ice-like shape was shown, whereas at 1.2C a liquid-like shape was shown, and at -4C, the film was intermediate between liquid-like and ice-like. AFM indicated that the adsorbed water

layer was flat and homogeneous. Studies examining the effect of pH have been conducted. All of these studies point to the conclusion that ordered hydrogen-bonding networks form at the interface between silicon and water.[20,21] As the thickness of the water layer increases, the structure becomes more similar to that of bulk liquid water.

## Water on Hydrophobic and Hydrophilic Surfaces

Hydrophobic surfaces have also been thoroughly researched. A common finding in previous studies is the adsorption of water in droplets at defects in hydrophobic surfaces. A study examining the adsorption of water on various laboratory surfaces found that the least water uptake occurred for the C8 SAM on borosilicate glass discs when compared to the other hydrophobic surfaces such as glass discs dipped or submerged in halocarbon wax and Teflon coatings.[3] The authors observed that the C8 SAM also had the fewest defects by examining the various surfaces with AFM (this was quantified by the surface average roughness). The FTIR data showed that the C8 SAM adsorbed smaller amounts of water, and the water peak was also red-shifted to 3200 $cm^{-1}$, indicating solid-like water. However, due to the uncertainty at in the appropriate infrared absorption coefficient in the water region and the small amounts adsorbed at low relative humidity, the authors were unable to ascertain whether the isotherms were Type II or Type III.

A similar study explored the correlation between the 3200 $cm^{-1}$ (solid-like) and 3400 $cm^{-1}$ (liquid-like) bands using molecular dynamic (MD) simulations, FTIR, and temperature-programmed desorption (TPD).[22] Silane SAMs on borosilicate glass of C8

alkane, C18 alkane, and C8 terminal alkene were tested. The C8 terminal alkene was also oxidized with KMnO4, which is reported to form a SAM terminated with COOH groups. The findings were similar to those in the previous study, where some water was adsorbed even for the hydrophobic surfaces. At 20% and 40% relative humidity for the C8 and C18 alkylsilane SAMs, FTIR showed a small peak around 3200 $cm^{-1}$. However, for 80% RH, contributions from the 3400 $cm^{-1}$ peak were also seen. After comparing these spectra with that of the uncoated substrate, the possibility that the adsorption was due to the penetration of water to the substrate was ruled out, due to a different shape and greater adsorption on the coated sample. MD simulations showed that with an increasing number of water molecules, the probability of water molecules forming three to four hydrogen bonds increased. Small water clusters were formed at low RH, and as humidity increased, the size of these clusters increased. Also, water molecules near the hydrophobic surface and the surface of the droplet exposed to the vapor phase were more likely to form one to two hydrogen bonds, whereas water molecules in the interior of the droplet were more likely to form three to four hydrogen bonds.

A different study that further probed the behavior of the water adsorption isotherm on hydrophobic surfaces was done by Rudich et al.[2] Instead of using spectroscopic techniques, this study utilized molecular controlled semiconductor resistor (MOCSER) and quartz crystal microbalance (QCM), which convert differences in signal to information about the mass of the adsorbed layers. The substrates tested were C18, C12, and C8 silane SAMs on crystals coated with plasma-deposited SiO2. The results showed that the water initially adsorbed at imperfections on the surface, which were far apart from each other, so the adsorption of water molecules on one site were independent

from the other sites. This follows the Langmuir model. The QCM data support the hypothesis that water adsorption beyond the first layer occurred on previously adsorbed water. Because MOCSER only measures adsorption on the first layer, the surface coverage is always less than a monolayer, and is not complete. The water adsorption was found to be reversible and dependent on relative humidity. MD simulations also agreed with the other studies and confirmed that water is in droplets for hydrophobic surfaces.

Hydrophilic surfaces have also been studied numerously. In the same study done by Moussa et al., when the C8= SAM was oxidized with $KMnO_4$ to a COOH terminal group, it was found that there was no clear increase in the amount of water adsorbed compared to the unoxidized SAM.[22] However, the TPD data showed that the activation energy for desportion of the oxidized SAM (44±5 kJ/mol) was higher than the activation energy of the unoxidized C8= SAM (40±6 kJ/mol) but lower than the reported value for a –COOH terminated thiol SAM (50 kJ/mol). These values are a good comparative measure of the relative strength of the interaction of water on the surface. Unlike the clustering of water molecules in one droplet in the hydrophobic case, MD simulations of –COOH terminated thiols showed small distributed clusters.

A similar MD study conducted by Szöri examined the wetting of hydrophobic (methyl-terminated) and hydrophilic (–COOH terminated) surfaces.[23] The study showed that there was a vast difference in water behavior for completely hydrophobic or hydrophilic sites. For the hydrophobic surface, water would form in droplets, and as water coverage increased, the size of the droplet increased. However, for the hydrophilic surface, small water clusters were spread out over the surface, eventually forming islands and covering the whole surface. Also, hydrogen bonding among the COOH groups

reoriented the end groups, and these terminal groups were more ordered in the presence of water, indicating the formation of hydrogen bonds with water molecules, and perhaps the breaking of H bonds between COOH groups.

Interfacial water studies were also done using forced dewetting of alkanethiols on Ag.[24] The residual ultrathin films resulting from the forced dewetting were analyzed using surface Raman spectroscopy and ellipsometry, which gave information about the molecular structure of interfacial water. By analyzing the v(O-D) modes, it was suggested that more ice-like character is present for –OH terminated surfaces, while more liquid-like character was seen for –COOH and $–CH_3$ terminated surfaces. Relatively strong water-carboxylic acid interactions were indicated by the thicker residual film observed relative to the –OH and $–CH_3$ terminated surfaces. The –OH terminated surface possesses both hydrophilic and hydrophobic character. Many of its polar hydroxyl groups are laterally hydrogen-bonded with neighboring hydroxyls into hydrophilic patches, but the methylene ($CH_2$) groups adjacent to the hydroxyl groups become exposed after the reorganization of the hydroxyl groups to facilitate hydrogen bonding. Each SAM surface indicated a distinct interfacial structure, and the observed water structure was very different from bulk water.

To observe the amount of water being adsorbed on alkanethiol SAMs, a study by Bertilsson et al. used a surface acoustic wave (SAW) sensor to observe the trend in the mass observed for $–CH_3$, –COOH, and –OH terminated SAMs on gold.[1] The $–CH_3$ terminated SAM showed about 1 monolayer of water coverage, while the –COOH surface showed 6 monolayers and the –OH surface showed 5.5 monolayers. The behavior

in frequency change for the –COOH and –OH surfaces were very similar and showed Type III trends.

## Proposed Techniques and Justification of Study

Water is present on virtually all surfaces due to atmospheric humidity. The interfacial properties of water have important implications in sensors,[1] the effects of organic substances in the atmosphere,[2,3] binding of biomolecules,[4] and nanotechnology. Because the behavior of interfacial water can have a significant impact on how a device behaves, it is important to investigate the behavior and structure of water on surfaces. Self-assembled monolayers (SAMs) are a useful tool because the terminal group can be controlled to produce many types of surfaces. SAMs have applications in a wide variety of fields, including biomimetic membranes, nano-scale photonic devices, solar energy conversion, catalysis, chemical sensing, and nano-scale lithography.[7] SAMs are widely used because they can be easily formed and provide a controlled surface. The surfaces investigated here were $–CH_3$, –COOH, and –OH terminated SAMs on gold. These functional groups are common, and understanding the structure and adsorption behavior of interfacial water on these individual components will lead to a better grasp of more complicated surfaces.

Interfacial water has been shown to have varying structure depending on the surface and environment studied.[1-3,5,6,21-26] Using attenuated total reflectance infrared spectroscopy (ATR-IR) on silicon oxide surfaces, it was found that water initially forms a solid-like structure, indicated by a peak at 3200 $cm^{-1}$ in IR spectra, but as the relative

humidity is increased, the adsorbed water transitions to a liquid-like state,[5,6,20,21] showing Type II adsorption behavior.[5,6] The first monolayer of adsorbed water is ordered in a solid-like manner due to the immobilized hydroxyl groups on the surface. Meanwhile, studies on hydrophobic surfaces have shown the presence of solid-like water at low relative humidity and liquid-like water at higher relative humidity.[22] Molecular dynamics (MD) simulations have also shown that small water clusters form on hydrophobic surfaces, and as water coverage increases, the size of the droplet increases.[22,23] However, for hydrophilic surfaces, small water clusters are distributed over the surface, eventually forming islands and covering the whole surface. The effect of relative humidity on the thickness of adsorbed water has not been studied extensively for SAMs, but it was observed using surface acoustic wave (SAW) that 5.5 and 6 monolayers of water formed at saturation on COOH and OH terminated SAMs, respectively.[1] Residual ultrathin films of $D_2O$ created after forced dewetting showed more ice-like structure on –OH terminated SAMs and more liquid-like water on $–CH_3$ and –COOH terminated SAMs.[24] Relatively strong water-carboxylic acid interactions were indicated by the thicker residual film observed relative to the –OH and $–CH_3$ terminated surfaces. Many of the –OH terminated polar hydroxyl groups were laterally hydrogen-bonded with neighboring hydroxyls into hydrophilic patches, but the methylene ($CH_2$) groups adjacent to the hydroxyl groups became exposed after the reorganization of the hydroxyl groups to facilitate hydrogen bonding.

Alkanethiol SAMs on gold were studied in this paper. While silane SAMs can be formed on silicon, they allow some water penetration to the substrate.[25] Alkylsilane SAMs on mica have also shown defects and portions of exposed mica showed humidity-

dependent changes.[26] Alkanethiol SAMs were chosen because the monolayers can be easily formed on gold by exposing it to the thiol dissolved in solution, have well-ordered packing,[27] and do not allow water to penetrate to the gold surface.[28] The easy control of surface chemistry through the terminal group also makes these SAMs a good choice of substrate.

Previous studies examining the structure of these surfaces in ambient conditions have been limited due to the challenges associated with probing the solid-fluid interface without interference from the bulk fluid.[24] While ATR-IR was a useful technique for studying silicon oxide, the refractive index of gold is small, and thus ATR-IR is only able to probe an extremely thin gold layer, and is not appropriate for this study. Instead, three different techniques were used to gain information about the behavior of interfacial water on these three surface chemistries. PM-RAIRS probes only the thiol SAM surface, and gives large signal from absorption, which is useful in detecting submonolayer to monolayer thicknesses. While PM-RAIRS gives useful information about the structure of the SAM and the adsorbed water, it is difficult to obtain thickness information quantitatively. QCM provides quantitative information about the total mass gain, but it cannot give insight onto the quality of the SAM or the structure of the adsorbed layer. Also, because it measures total mass gain, including the mass of water adsorbed on the quartz surface, QCM cannot give an accurate value for the thickness of the water layer on the gold surface, which can be related to the mass gain by using the Sauerbrey equation. Ellipsometry measures the thickness of the adsorbed water, but does not give structural information. However, combining these three techniques can give a clearer picture of the structure and behavior of adsorbed water, which can be compared among three different

functional groups, $–CH_3$, –COOH, and –OH, and ultimately with the silicon oxide surface.

This study seeks to quantify the actual thickness and determine the structure of adsorbed water on $–CH_3$ (1-hexadecanethiol), –COOH (12-mercaptododecanoic acid), and –OH (11-mercapto-1-undecanol) terminated alkanethiol SAMs on gold. This paper elucidates the structural data obtained from PM-RAIRS. The 11-mercapto-1-undecanol bulk spectrum is used along with ellipsometry data to determine the relationship between –OH and $–CH_2$ peak intensity. Thickness estimates are obtained using this relationship and the PM-RAIRS spectra. The interfacial behavior of water determined by the data on these three surfaces is compared with ATR-IR data on $SiO_2$, and the usefulness of each technique is examined.

## Chapter 2

# Water Adsorption on $-CH_3$, –COOH, and –OH terminated SAMs

The behavior of water on $-CH_3$, –COOH, and –OH terminated SAMs was investigated using PM-RAIRS, QCM, and ellipsometry. The $-CH_3$ terminated SAM shows no adsorption of water due to the hydrophobic nature of the methyl group. The adsorption isotherm of water on the –COOH terminated SAM shows a strong humidity dependence. Also, broad OH stretching peak indicates a distribution of liquid-like and solid-like structures. Some of the COOH groups ionize to COO–, which could cause a stronger water-surface interaction. The –OH terminated SAM keeps a large amount of water molecules on it even at dry conditions and the adsorption isotherm exhibits little humidity dependence. The OH stretching peak is more narrow and shows a larger contribution from liquid-like water.

## Experimental Methods

### Sample Preparation for PM-RAIRS and Ellipsometry

Gold-coated silicon was allowed to sit in 20 mM solutions of 1-hexadecanethiol (Fluka Chemika), 12-mercaptododecanoic acid (Aldrich, 96%), and 11-mercapto-1-undecanol (Aldrich, 97%) in ethanol (Pharmco-Aaper, 200 proof) for 30 minutes. Previous studies employed 1-2 mM concentrations with overnight adsorption.[24,29] However, it has been shown that as the concentration increases, adsorption time is faster,[30-32] so higher concentrations were tested. Concentration and time experiments

were performed, and PM-RAIRS showed that 20 mM solution and 30 minute adsorption time produced the best packing on these gold surfaces. It was also found that new gold samples allowed for better thiol adsorption. Figure 1 shows the time dependence tests that were run using PM-RAIRS on the COOH and OH SAMs.

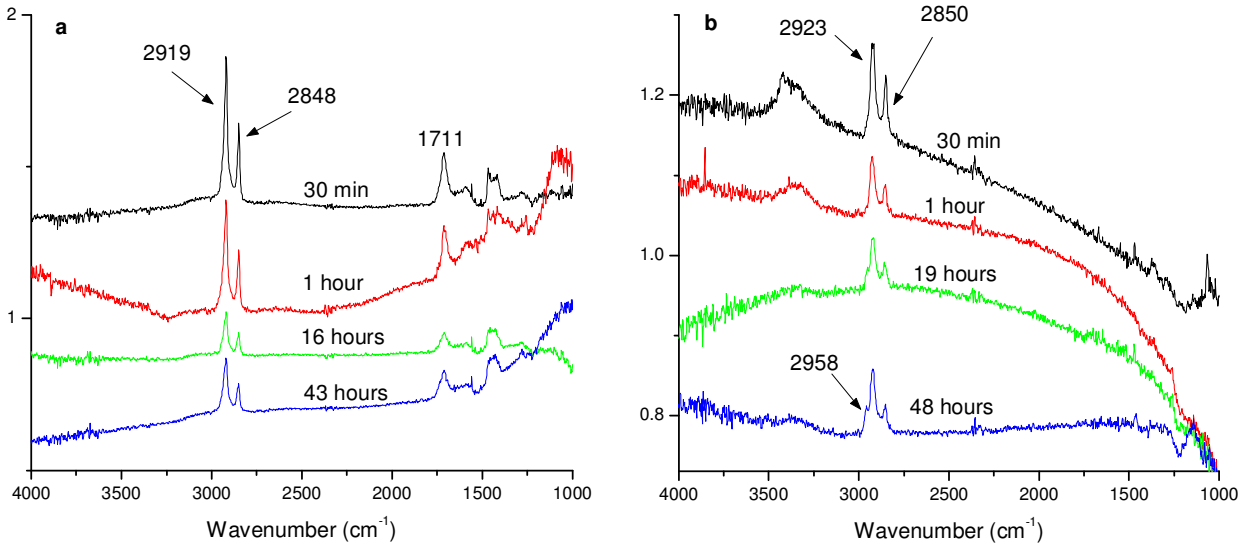


Figure 1: Time dependent tests for COOH and OH SAMs
(a) PM-RAIRS of 12-mercaptododecanoic acid SAM after varying amounts of time. (b) PM-RAIRS of 11-mercapto-1-undecanol after varying amounts of time. Both of these spectra were first divided by the original gold spectra.

For the COOH SAM, the 30 minute adsorption time produced the best intensity for both the CH2 stretching and C=O stretching peaks. The peak positions for $CH_2$ symmetric and asymmetric stretching modes were 2848 $cm^{-1}$ and 2919 $cm^{-1}$, respectively, while the C=O peak appeared at 1711$cm^{-1}$. It has been demonstrated that for well-packed SAMs the $\upsilon_{sy}(CH_2)$ is at 2848 $cm^{-1}$ and $\upsilon_{as}(CH_2)$ is at 2917 $cm^{-1}$. However, for more disordered monolayers, these absorptions occur at ~2856 and 2923 $cm^{-1}$, respectively.[33-35]

For the OH SAM, once again the 30 minute adsorption time produced the highest

intensity peaks. After longer adsorption times, a $CH_3$ stretching peak began to appear at 2958 $cm^{-1}$, and the OH peak begins to diminish, signaling degradation of the SAM. The peak positions for $CH_2$ symmetric and asymmetric stretching modes were 2850 $cm^{-1}$ and 2923 $cm^{-1}$, respectively, indicating a slightly more disordered monolayer than COOH. The intensity of the $CH_2$ stretching peaks was greater for the COOH SAM, along with the signal-to-noise ratio. The COOH SAM also showed very little water adsorbed at dry conditions, whereas the OH SAM already showed a broad water peak (3600 $cm^{-1}$ to 3000 $cm^{-1)}$ at dry conditions. The 30 minute adsorption time was enough to produce well-packed SAMs, and gave better spectra than the SAMs that were in solution longer, which was not found to be true for 1-2 mM concentrations. Bain et al. showed that at these moderate concentrations, the adsorption process was characterized by two phases: rapid adsorption and slower consolidation.[32] Within a few minutes, the SAM reached about 80-90% of its maximum thickness. The slower process allows additional adsorption, possibly involving displacement of contaminants and lateral diffusion on the surface to reduce defects and enhance packing. This was not observed for higher concentrations, as longer adsorption times produced more disordered SAMs. The water contact angle for the $CH_3$ SAM was 120°, and <10° for both the COOH and OH SAMs.

Figure 2 shows the bulk spectra for the three thiols. The bulk spectrum for the OH SAM, which is seen in Figure 2(c), was used to determine how much of the OH stretching peak was due to the alcohol group of the thiol. The ratio of the OH peak (1) over the $CH_2$ peak (2) was 0.5 for the bulk spectrum.

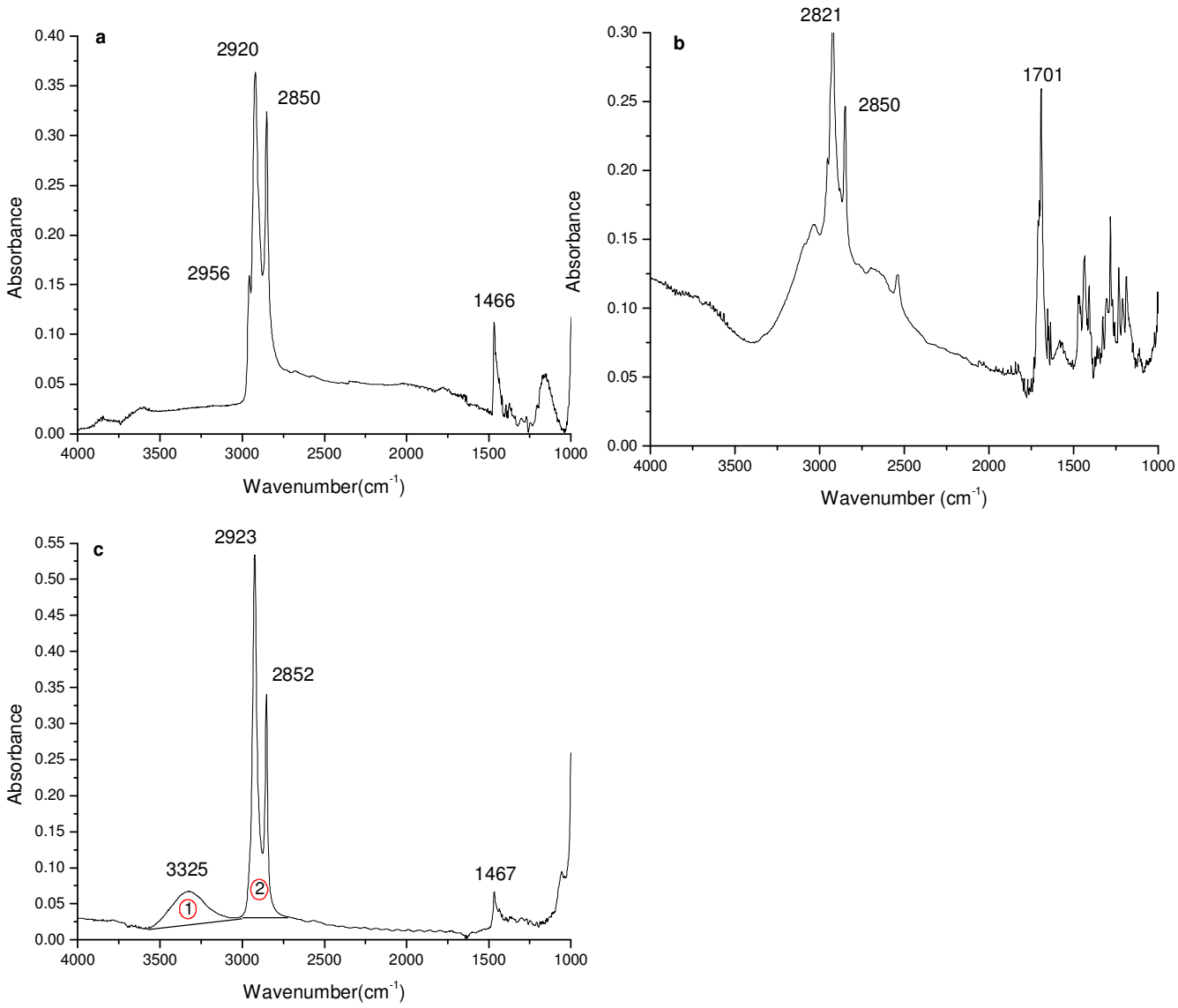


Figure 2: Baseline corrected bulk thiol transmission spectra
(a) 1-hexadecanethiol (b) 12-mercaptododecanoic acid (c) 11-mercapto-1-undecanol.

**PM-RAIRS**

The relative humidity was regulated using argon and water bubblers. Data was collected using a Thermo-Nicolet Nexus 670 spectrometer with a liquid nitrogen cooled

MCT detector, a photoelastic modulator (HINDS Instruments PEM-90), a demodulator (GWC Instruments), and Omnic software. The gain was set at 1, with 200 scans. Gold samples (8 mm by 2 cm) were cleaned with oxygen-argon plasma (20 cycles) and were put in 20 mM thiol solution for 30 minutes. The sample was then rinsed with ethanol for 10 seconds, dried with argon, and placed in a sample holder within a chamber. The chamber was closed and connected to the inlet gas stream. Dry argon was blown through the chamber until the signal was shown to be steady, and spectra were taken in increments of 10% relative humidity. After the flows of argon and saturated water vapor were adjusted, the sample was allowed to equilibrate for 5 minutes before the next reading was taken. Figure 3 shows the set up of PM-RAIRS system. The IR beam was sent through the photoelastic modulator, with an angle of incidence of 81° to the sample. The angle between the incident IR beam and the detector is around 18°. The sample angle was adjusted until the maximum through-put was achieved.

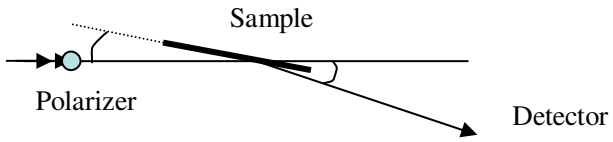


Figure 3: PM-RAIRS set up.

## QCM

### *Sample Preparation*

5 MHz QCM crystals (Tangidyne TAN05RCBG, 14mm) made of quartz and covered with gold were used. Thiols do not adsorb to the quartz surface, so two different methods were employed to account for quartz's hydrophilic nature.

#### *Method I: Hydrophobitizing the back side with hexamethyldisilazane (HMDS)*

HMDS is a volatile liquid with hydrophobic groups. In order to prepare a HMDS-treated sample, the front and back side of the quartz crystal was first plasma treated and placed in a 20 mM CH3 thiol solution for 30 minutes. After the crystal was taken out, it was rinsed with ethanol, dried with argon, and placed in a sealed petri dish with a small amount of HMDS. The sample was allowed to sit overnight to allow the HMDS to vaporize onto the quartz. Afterwards, the front side was again treated with plasma, and placed in the thiol solution to be tested. Using this method, it was presumed that the back side was hydrophobic and water adsorption was occurring on the front side only.

#### *Method II: Allow the quartz to adsorb water*

The samples using this method were plasma treated on both the front and back side, placed in a 20 mM $CH_3$ thiol solution for 30 minutes, rinsed with ethanol, and dried

with argon. The front side was then treated with plasma again and placed in the thiol solution to be tested. Using this method, it was assumed that the frequency change for the CH3 sample will yield the "amount" of water being adsorbed by the quartz, since it was shown that CH3 does not adsorb very much water. This "amount" was then subtracted from the frequency changes for the two hydrophilic SAMs.

***QCM Methods***

Once the sample was prepared, it was placed in the sample holder and then in the QCM chamber. The measurements were taken by Stanford Research Systems Model QCM200. A thermocouple was placed in the sample holder to monitor the temperature of the sample. The chamber was sealed, and had an inlet and outlet to introduce the saturated vapor. The chamber was blown with argon until the frequency reached steady state. Saturated vapor was then introduced at a flow rate of 10 sccm/min, and the time was recorded. QCM is very sensitive to temperature changes and disturbances in flow at the surface. However, it was found that at the frequency did not change when this flow was introduced. The resistance decreased slightly during the gap when the two flows were switched. A complete mixing model was used to determine the relative humidity as a function of time. The experiment was stopped after one hour (about 4 residence times), corresponding to 98.7% relative humidity.

**Ellipsometry**

An ellipsometer (EllipsoTech SWE, wavelength = 632.8 nm, incidence angle = 69.3$^{o}$) was used to measure the film thickness. The refractive index of the –$CH_3$, –COOH, and –OH terminated SAMs (1.46, 1.55, 1.52, respectively) were used along with the refractive index of gold (0.13) to calculated the film thickness. The refractive index of water (1.33) was used to measure the water adsorption onto the various SAMs.

## Results and Discussion

Figure 4(a) shows the adsorption spectra for the –$CH_3$ terminated SAM. The amount of water adsorbed is minimal and does not change with increasing humidity, as there is no change in the OH peak intensity. The water adsorption isotherm, shown in Figure 4(b), was determined by integrating the OH and $CH_2$ stretching peaks and taking the ratio. Figure 4 shows that as saturation is reached, more water does not adsorb to the surface.

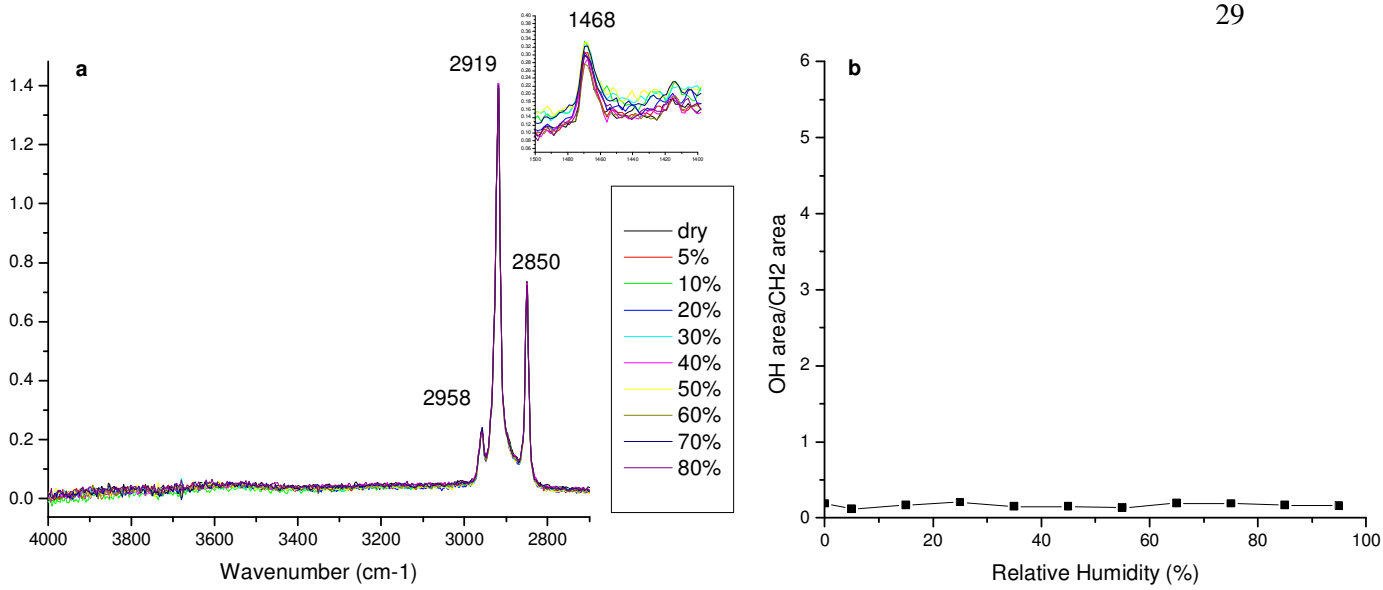


Figure 4: (a) PM-RAIRS spectra of 1-hexadecanethiol. (b) The ratio of the area of the water peak over the area of the $CH_2$ and $CH_3$ stretching peaks.

Although COOH and OH are both hydrophilic surfaces, the adsorption isotherm looks different for the two cases. Figure 5 shows the PM-RAIRS spectrum and water adsorption isotherm for the –COOH terminated SAM. The COOH spectrum shows a broad water peak, indicating several types of OH environments. Solid-like and liquid-like water are characterized by peaks in the OH stretching vibration region at 3230 $cm^{-1}$ and 3400 $cm^{-1}$.[5,20] The broad peak in Figure 5(a) indicates that the adsorbed water exists in both solid-like and liquid-like structures. Very little water was adsorbed at dry conditions, but as the humidity increased, the amount of water adsorbed also increased, showing exponential Type III behavior and strong humidity dependence. The presence of ionized groups, shown in Figure 6, could have an effect on why the amount of water adsorbed is so large and the different structure of the interfacial water from bulk liquid water.

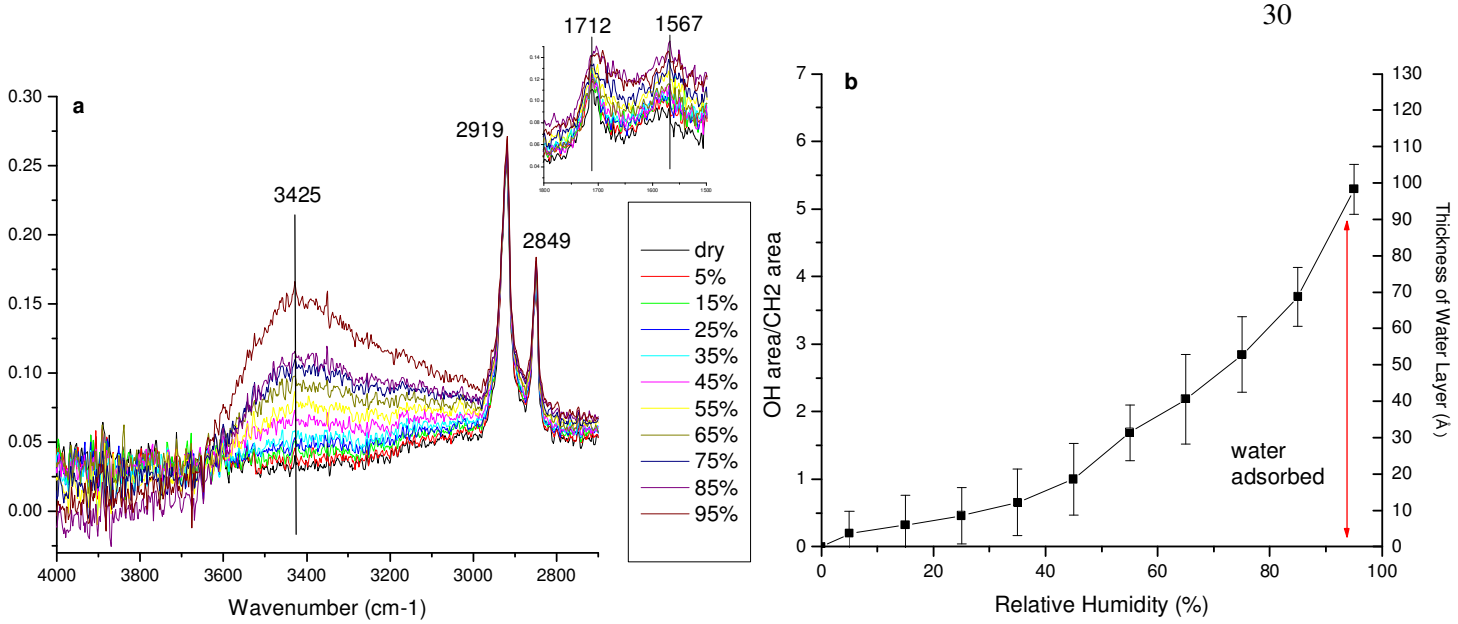


Figure 5: (a) PM-RAIRS spectra of 12-mercaptododecanoic acid. (b) The ratio of the area of the water peak over the area of the CH2 stretching peaks.

The thickness of the adsorbed water layer was estimated by finding the approximate thickness of 11 $CH_2$ groups and multiplying the normalized area of the OH peak to this thickness. The normalized area is the area of the OH stretching peak divided by the area of the $CH_2$ peak, which is due to contributions from 11 $CH_2$ groups. Ellipsometry experiments of 1-hexadecanethiol on gold measured the $C_{16}$ SAM to be 2.7 nm. This data, along with the normalized OH peak intensity from the bulk spectra, was used to find the thickness of the water layer:

$$\frac{2.7nm}{16CH_2}\cdot 11CH_2\cdot(normalized\ area\ OH\ peak)=1.86nm*normalized\ area \qquad [2]$$

If the normalized area is 1, the thickness of the water layer is estimated to be 18.6 Å.

Figure 6 shows the lower wavenumber region of the $CH_3$ and COOH spectra. The $CH_3$ spectrum shows only the 1468 $cm^{-1}$, which is due to the $CH_2$ bending or scissoring vibration.[36,37]

Figure 6(b) shows that the COOH spectrum contains multiple peaks. The 1467 $cm^{-1}$ peak in the COOH spectrum is much broader than that seen in the $CH_3$ spectrum. It has been shown that COO– symmetric stretching vibration occurs around 1390 to 1410 $cm^{-1}$.[36,39,40] The 1711 $cm^{-1}$ peak shown in the dry spectrum is indicative of the C=O stretching vibration from the carboxylic acid group, which has been shown to appear around 1700 $cm^{-1}$ to 1730 $cm^{-1}$.[36-39] However, there is also a peak at 1577 $cm^{-1}$. The COO– group also has an asymmetric stretch around 1575 $cm^{-1}$.[39] Therefore it is likely that the peaks observed are a result of ionized COOH groups. The 95% relative humidity spectrum shows increases and shifts in the 1711 $cm^{-1}$ and 1577 $cm^{-1}$ peaks, indicating a transition of the COOH groups to ionized COO– groups. The 1672 $cm^{-1}$ peak shown in the subtracted spectrum is from the water bending vibration, and shows the growth of the water layer on the surface.

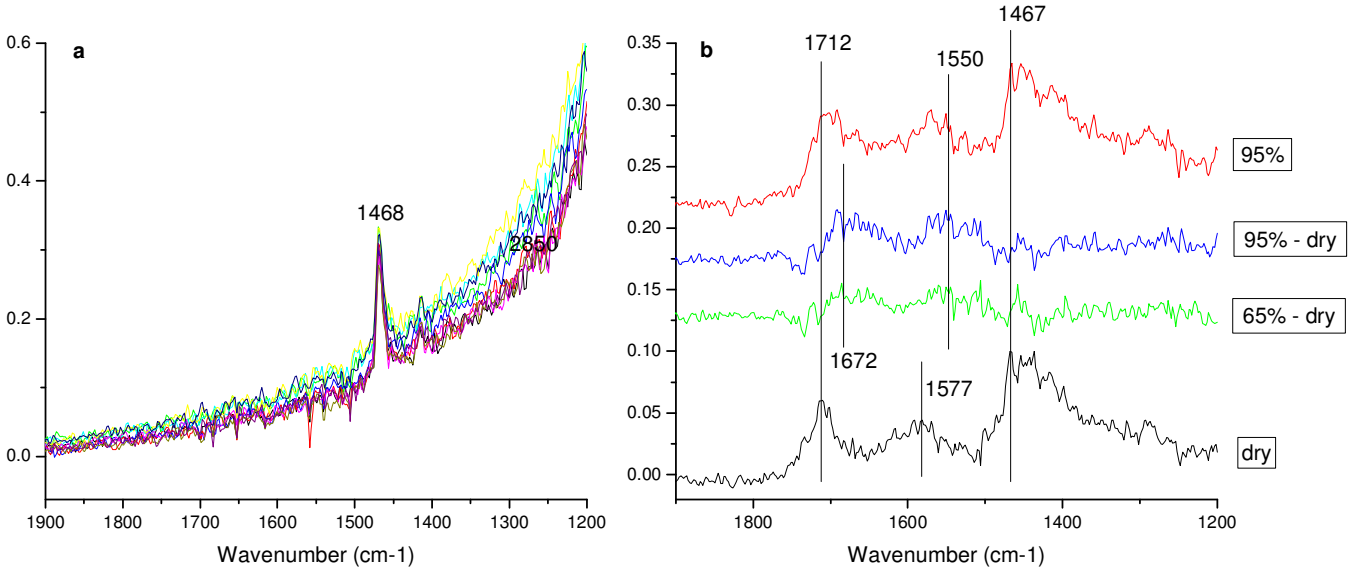


Figure 6: PM-RAIRS spectra for (a) $-CH_3$ terminated SAM and (b) dry and 95% relative humidity –COOH terminated SAM, the dry spectrum subtracted from the spectrum at 65% relative humidity, and the dry spectrum subtracted from the spectrum at 95% relative humidity.

The water peak for the OH spectrum shown in Figure 7(a) is a contrast to the broad peak in Figure 5(a). The peak position of the OH stretching vibration appears around 3400 $cm^{-1}$ for both hydrophilic SAMs, which is associated with liquid-like water. It appears that there is only a small contribution around 3200 $cm^{-1}$ for the OH SAM, suggesting that overall the structure of the water is more disordered. This could be because the surface groups on the SAM are more disordered than the immobilized hydroxyl groups that are found on silicon oxide.

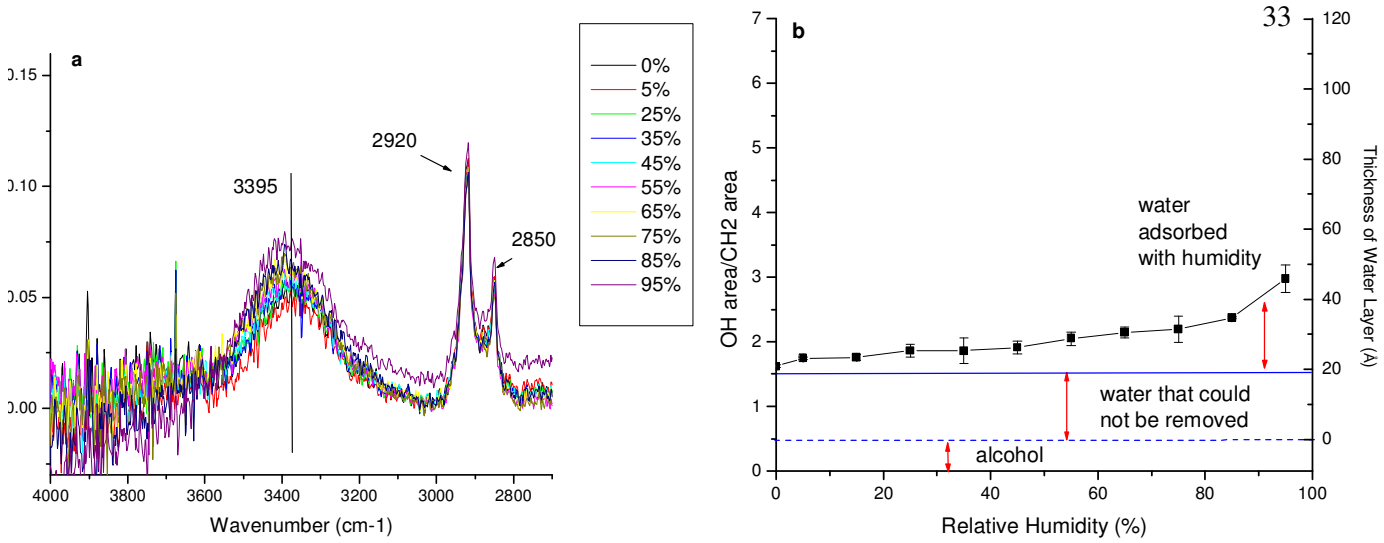


Figure 7: (a) PM-RAIRS of 11-mercapto-1-undecanol. (b) The ratio of the area of the water peak over the area of the $CH_2$ stretching peaks.

The OH SAM displayed a large amount of adsorbed water that could not be removed, even after considerable drying. In further efforts to remove the water, the cell was heated up to 70°C while blowing argon, but this did not result in smaller water peak intensity. The cell could not be heated further without damaging the SAM. The isotherm shows a very shallow increase in the amount of water adsorbed on the surface. This is due to the large amount of water initially adsorbed to the surface.

The bulk spectrum for the OH SAM, which is seen in Figure 2(c), was used to determine how much of the OH stretching peak was due to the alcohol group of the thiol. The ratio of the OH peak (1) over the $CH_2$ peak (2) was 0.5 for the bulk spectrum. Thus, in Figure 7(b), the amount of the OH peak which is from the alcohol is drawn in at 0.5. Since the total normalized area of the water peak was 1.5, two-thirds of the peak is due to the water adsorbed at dry conditions. The approximate thickness of the water layer that could not be removed was calculated using Equation 1, and resulted in an initial thickness

of 18.6 Å. The water adsorption isotherm for silicon oxide has been observed to show Type II behavior.[5,6] Figure 8 shows the water adsorption isotherm obtained by Asay and Kim.[5] The thickness of the water layer that could not be removed, 18.6 Å, would intersect the adsorption isotherm at 90% relative humidity, which is well above the transition region that defines the Type II isotherm, as seen in Figure 8. At this point, about 3 additional monolayers, or 9 Å, adsorbed to the $SiO_2$. However, for the OH SAM, the water layer grows to about 45 Å thick, which is an addition of about 8 monolayers of water.

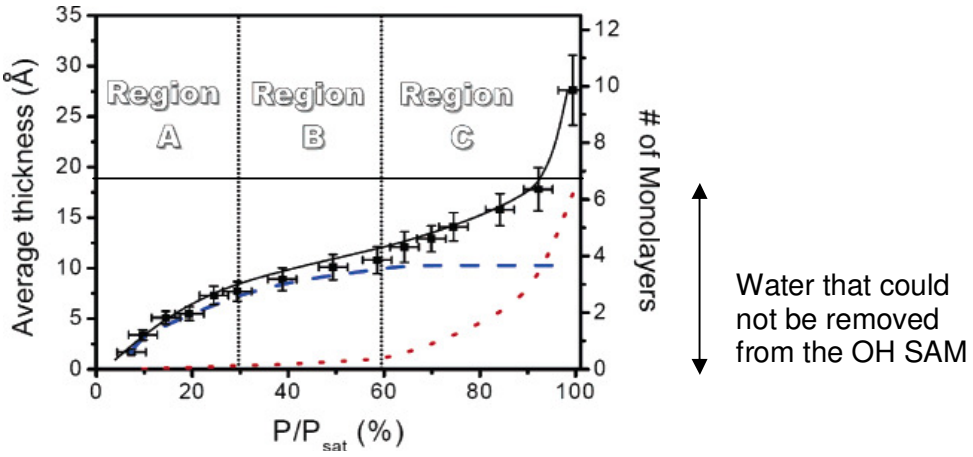


Figure 8: Adsorption isotherm of water on the silicon oxide surface (Asay, 2005). The line at 18.6 Å shows how much water is initially adsorbed on the OH SAM.

Although the overall thickness of the water layer on the OH SAM is greater than that seen on the silicon oxide surface, the layer grows more gradually due to the amount of water initially adsorbed to the surface.

The QCM data shown in Figure 9 verifies the trends seen from PM-RAIRS. However, some differences were seen due to the quartz surface and back side of the

crystal. Even after hydrophobitizing the back side with HMDS, the $CH_3$ sample still showed considerable water adsorption. The contact angles were measured for the front side, back side gold, and back side quartz, and were >90°, 80°, and 70°, respectively for the $CH_3$ sample. There was very little change in mass until around 70% relative humidity, indicating that nucleation of small water droplets could have occurred here, resulting in more water adsorbing to these sites. A completely hydrophobic surface will have contact angles greater than 90°, and it is likely that some water adsorbed on the back side, making the frequency change not due completely to adsorption on the SAM.

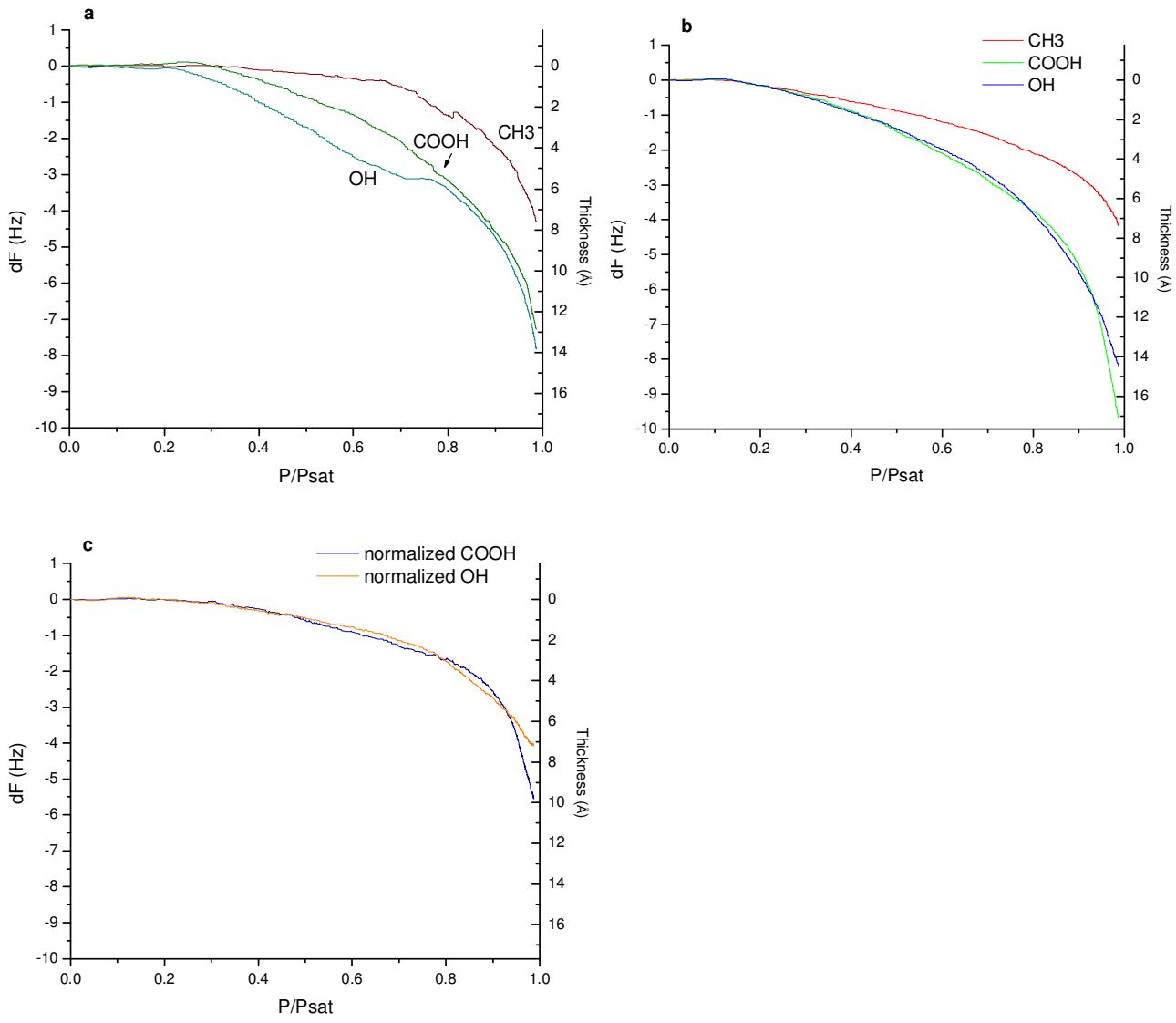


Figure 9: (a) Change in frequency for samples prepared using HMDS to hydrophobitize the back side of the crystal. (b) Change in frequency for samples prepared without treating the quartz with HMDS. (c) The change in frequency after subtracting the change in frequency curve for the CH3 sample from the COOH and OH samples from (b).

Because of results obtained from PM-RAIRS, which showed little to no adsorption of water on the $CH_3$ SAM, it was presumed that any water adsorbed using Method II would result from adsorption on the back side of the crystal. After subtracting

the change in frequency from this adsorption, the shapes of the COOH and OH curves look slightly different, as seen in Figure 9(c). The OH curve displays a slower increase in adsorption of water, while the amount of water adsorbed on the COOH SAM is once again greater than the OH SAM. The results from the two preparation methods show similar trends, with increase in the mass of water adsorbed occurring around 80% relative humidity. The thickness estimate obtained from QCM using the Sauerbrey equation for the OH SAM is close to what would be expected from the $SiO_2$ data that was previously discussed. The QCM data estimates a 7 Å increase in thickness, while the $SiO_2$ data shows about a 9 Å increase would be expected.

A similar adsorption experiment was done using SAW by Bertilsson et al. Even after correcting for the bare, hydrated quartz, the $CH_3$ SAM showed about one monolayer of adsorbed water, COOH showed about 6 monolayers, and OH showed about 5.5 monolayers of adsorption.[1] If the Sauerbrey equation is used to calculate the thickness of the adsorbed water, the $CH_3$ SAM prepared using Method I shows about 2 monolayers of coverage, while the $CH_3$ SAM prepared using Method II shows about 3 monolayers of coverage. The COOH SAM showed about 5 monolayers using Method I and 7 monolayers using Method II (without subtracting the CH3 frequency change), and the OH SAM showed about 5.5 monolayers using both methods. It seems likely that water adsorption on both the $CH_3$ SAM as well as on the quartz contributes to the mass change detected by QCM. The SAW data also showed that increases in the mass of water adsorbed occurred around 80% relative humidity, and the –COOH terminated SAM adsorbed more water than the –OH terminated SAM. Similar adsorption behavior for $SiO_2$ was seen if the initial amount of water adsorbed to the OH surface is accounted for.

While the trends observed were similar to what was seen in PM-RAIRS, quantitatively, QCM shows a smaller thickness of adsorbed water. This could be due to the low quality factor of the sample or the inaccuracy of the approximated thickness found by PM-RAIRS.

Ellipsometry gives thickness information by measuring the change of polarization as given by the parameters delta and psi. Ellipsometry probes the thiol surface, but the difference in refractive index between the gas phase and the adsorbate phase is small, and the laser had problems with instability and electrical grounding, so the sensitivity was small. The actual thickness of the adsorbed water layer could not be determined. Figure 10 shows how delta changes with the addition of a 2 nm SAM and 40 Å of water according to the model. With 20 Å of adsorbed water, delta is expected to change 1.2 or 1.3°. However, these changes in delta were not seen by the ellipsometer due to the problems with the laser. These experiments will be redone with a new laser, but could not be completed in time for this paper.

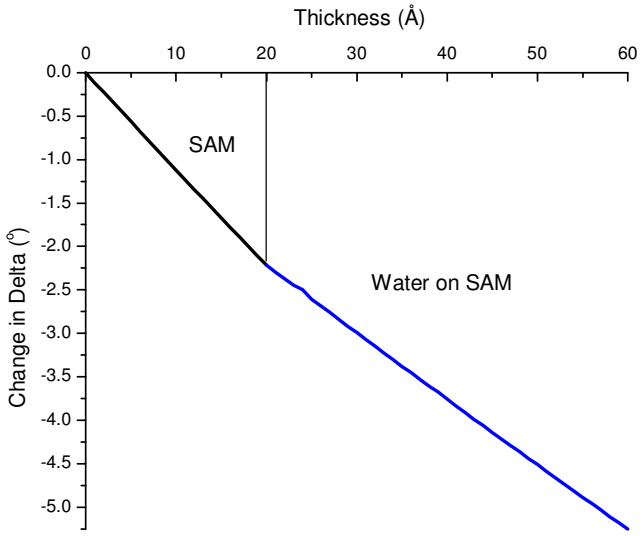


Figure 10: Change in Delta vs. thickness of SAM and water layer.

Although the measured changes in delta with relative humidity, Figure 11, cannot be directly converted to thickness, they do give a good idea of what the adsorption isotherm looks like. The trends in the adsorption isotherms are similar to those shown by the PM-RAIRS data. The $CH_3$ SAM adsorbs little water, the COOH SAM behavior shows a strong humidity dependence, and the OH SAM shows little uptake until high partial pressures are reached. The behavior shown by ellipsometry verifies the trends seen by PM-RAIRS and QCM.

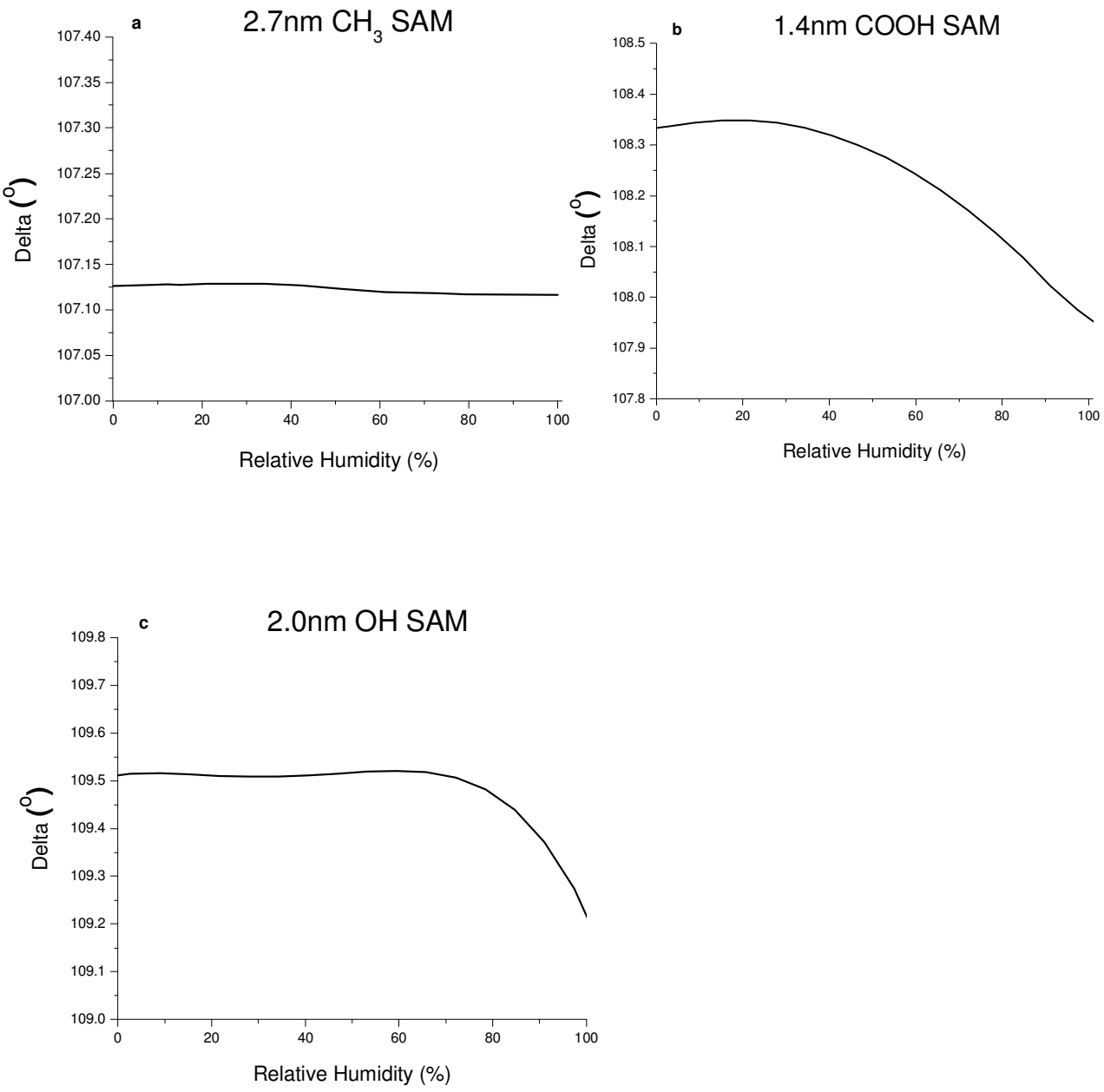


Figure 11: Change in Delta for (a) 1-hexadecanethiol (b) 12-mercaptododecanoic acid (c) 11-mercapto-1-undecanol.

## Conclusion

After examining $–CH_3$, –COOH, and –OH terminated SAMs using PM-RAIRS, QCM, and ellipsometry, it was shown that each technique gave similar trends in the adsorption of water. The $CH_3$ surface adsorbed little water with increasing partial pressures, while the COOH SAM showed a gradual increase. The OH SAM showed a large amount of water that could not be removed in dry conditions, and this water thickness was steady until high partial pressures were reached. The adsorbed water on the COOH showed a broad distribution of OH environments, indicating the presence of solid-like and liquid-like water. Water on the OH SAM showed more liquid-like structure. PM-RAIRS is useful because it shows the quality of the SAM and the structure of the adsorbed water layer. Although it does not give an exact thickness, PM-RAIRS data can give a rough thickness estimate when combined with ellipsometry. Ellipsometry and QCM verify the trends seen with PM-RAIRS, but due to the sensitivity of these instruments, the substrate used, and the small scale of water adsorbed, these data should be mainly taken as qualitative. The adsorption behavior of water on each of these surfaces is very different, and has profound effects in the areas of sensing, nanotechnology, and binding of biomolecules.

## Future Work

Further experiments with ellipsometry will be performed using a new laser to obtain better thickness estimates. Other techniques to characterize water adsorption can be investigated, such as SAW. Future work can move towards examining the adsorption of other molecules, such as alcohols, or the characterization of other substrates, such as biomolecules, which are largely composed of the functional groups that were studied here.

## References


1. Bertilsson, L.; Potje-Kamloth, K.; Lieww, H.-D.; *Langmuir*, **1999**, *15*, 1128.
2. Rudich, Y. et al. *J. Phys. Chem. A* **2000**, *104*, 5238.
3. Sumner, A. et al. *Phys. Chem. Chem. Phys.*, **2004**, *6*, 604.
4. Senaratne, W.; Andruzzi, L.; Ober, C. *Biomacromolecules*, **2005**, *6*, 2427.
5. Asay, D.; Kim, S. H. *J. Phys. Chem. B*. **2005**, *109*, 16760.
6. Verdaguer, A. et al. *Langmuir*, **2007**, *23*, 9699.
7. Vos, J.; Forster, R.; Keyes, T.; *Interfacial Supramolecular Assemblies*; Wiley: West Sussex, England, 2003.
8. Ulman, A. *Chem. Rev*. **1996**, *96*, 1533.
9. *Introduction to Fourier Transform Infrared Spectroscopy*. Madison: Thermo Nicolet, 2001.
10. Hsu, C. P. *Handbook of Instrumental Techniques for Analytical Chemistry*, Prentice-Hall: New Jersey, 1997.
11. Urban, M. W. *Attenuated Total Reflectance Spectroscopy of Polymers Theory and Practice*; American Chemical Society: Washington, DC, 1996.
12. "What Is PM-IRRAS?" *Keck Interdisciplinary Surface Science Center*. NUANCE, 2009. Web. 24 Feb. 2010.
13. H. Fujiwara, *Spectroscopic Ellipsometry: Principles and Applications*, John Wiley & Sons Inc (2007).
14. Naaman, Ron. *Molecular Controlled Semiconductor Devices Abstract*. Proc. of American Physical Society Annual March Meeting, Minneapolis.
15. McGovern, M. E.; Kallury, K. M. R.; Thompson, M., *Langmuir*, **1994**, *10*, 3607.
16. Bierbaum, K.; Kinzler, M.; Wo¨ll, Ch.; Grunze, M.; Hahner, G.; Heid, S.; Effecberger, F., *Langmuir*, **1995**, *11*, 512.
17. Nakagawa, T.; Ogawa, K., *Langmuir*, **1994**, *10,* 367.
18. Bierbaum, K.; Grunze, M. *Adhes. Soc.* **1994**, 213.
19. Barnette, Anna L. *Adsorption Isotherm and Average Orientation of Adsorbed Alcohol and Water Layers on SiO2 in Ambient Conditions*. Diss. The Pennsylvania State University, 2008.
20. Du, Q.; Freysz, E.; Shen, Y.R.; *Phys. Rev. Lett.*, **1994**, *72*, 238.
21. Ostroverkhov, V.; Waychunas, G.; Shen, Y.R.; *Chem. Phys. Lett.*, **2004**, *386*, 144.
22. Moussa, S. et al. *J. Phys. Chem. A*, **2009**, *113*, 2060.
23. Szöri, M.; Tobias, D.; Roeselová, M. *J. Phys. Chem. B*, **2009**, *113*, 4161.
24. Tiani, D.; Yoo, H.; Mudalige, A.; Pemberton, J. *Langmuir*, **2008**, *24*, 13483.
25. Lane, J.; Chandross, M.; Lorenz, C.; Stevens, M.; Grest, G.; *Langmuir*, **2008**, *24*, 5734.
26. Díez-Pérez, I. et al. *Langmuir*, **2004**, *20*, 1284.
27. Porter, M. D.; Bright, T. B.; Allara, D. L.; Chidsey, C. E. D. *J. Am. Chem. Soc.* **1987**, *109*, 3559.
28. Asay, D. B.; Barnette, A. L.; Kim, S. H.; *J. Phys. Chem. C* **2009,** *113,* 2128–2133.
29. Engquist, I.; Lestelius, M.; Liedberg, B., *J. Phys. Chem.* **1995**, *99*, 14198.
30. Peterlinz, K. A.; Georgiadis, R. *Langmuir*, **1996**, *12*, 4731-4740.
31. Dannenberger, O.; Buck, M.; Grunze, M.; *J. Phys. Chem. B* **1999**, *103*, 2202.
32. Bain, C. et al. *J. Am. Chem. Soc.* **1989**, *111*, 321-335.
33. Angst, D. L.; Simmons, G. W. *Langmuir* **1991**, *7*, 2236.
34. Zhang, Q.; Zhang, Q.; Archer, L. A. *J. Phys. Chem. B* **2006**, *110*, 4924.

35. Dubowski, Y.; Vieceli, J.; Tobias, D. J.; Gomez, A.; Lin, A.; Nizkorodov, S. A.; McIntire, T. M.; Finlayson-Pitts, B. J. *J. Phys. Chem. A* **2004**, *108*, 10473.
36. Imae, T.; Torri, H. *J. Phys. Chem. B* **2000**, *104*, 9218.
37. Salmain M.; Fischer-Durand, N.; Roche, C.; Pradier, C.; *Surf. Interface Anal.* **2006**, *38*, 1276.
38. Langner, R.; Zundel, G.; *J. Chem. Soc.* **1995**, *91(21)*, 3831.
39. Bieri, M.; Bürgi, T.; *Langmuir*, **2005**, *21*, 1354.
40. Bieri, M.; Bürgi, T.; *J. Phys. Chem. B* **2005**, *109*, 22476.

# ACADEMIC VITA

**Aimee Tu**
**216 Highland Ave**
**Devon, PA 19333**
**emerocy@gmail.com**

## EDUCATION

THE PENNSYLVANIA STATE UNIVERSITY, University Park, PA

### B.S. in Engineering Science, May 2010

**B.S. in Chemical Engineering, May 2010**

The Schreyer Honors College

Thesis Title: Water Adsorption and Characterization on Alkanethiol Self-assembled Monolayers on Gold

Thesis Supervisor: Seong H. Kim

## EXPERIENCE

**Undergraduate Research at Penn State** Fall 2008/Present

*Honors Thesis, Schreyer Honors College*

Conduct experiments investigating water adsorption on self-assembled monolayers. Presented poster at 2009 AIChE Annual Meeting (Interfacial Phenomena poster session).

**Undergraduate Research at The University of Queensland in Australia** Summer 2009

*Research Experience for Undergraduates sponsored by the National Science Foundation*

Performed research on the separation of methane and nitrogen using temperature swing adsorption. Designed experiments, wrote a research paper, and presented results.

**Undergraduate Research at The University of Arizona** Summer 2008

*Research Experience for Undergraduates sponsored by the National Science Foundation*

Performed research on the adsorption of arsenic on magnetite. Worked directly with the faculty, wrote a research paper, and presented results.

**Intern at National Nano Device Laboratories in Taiwan** Summer 2007

*Taiwan Tech Trek program*

Performed research on photonic crystal sample fabrication and presented results. Collaborated with a diverse group of engineers and broadened global perspective.

**Facilitator of Study Group** Spring 2007

*Women in Engineering Program (WEP)*

Conducted a study group to help women engineers acquire greater knowledge in the subject of linear algebra and matrix operations. Counseled attendees and helped them develop problem-solving skills.

## ACTIVITIES/LEADERSHIP

| | |
|---|---|
| Asian American Christian Fellowship | Vice President, Retreat Head, Small Group Leader |
| Women in Engineering Program | Facilitator, Member |
| Knowledge, Excellence, Wisdom, and Learning Mentoring Program | Mentor |
| Pennsylvania Governor's School for the Sciences 2005 | Participant |

## AWARDS/ HONORS

Dean's List (Semester GPA above 3.50) – Fall 2006 to Fall 2009
Larry Duda Undergraduate Student Research Award – Department of Chemical Engineering
Paul Morrow Endowed Scholarship – Penn State College of Engineering
McNitt Scholarship in Engineering
Academic Excellence Scholarship – Schreyer Honors College
National Merit Scholarship Corporation - Finalist
Sanofi-Aventis Academic Achievement Scholarship